CORRIGENDUM

ANDREW HEYMSFIELD

National Center for Atmospheric Research, Boulder, Colorado

MIKLÓS SZAKÁLL AND ALEXANDER JOST

Institute for Atmospheric Physics, Johannes Gutenberg University, Mainz, Germany

IAN GIAMMANCO

Insurance Institute for Business and Home Safety, Richburg, South Carolina

ROBERT WRIGHT

RLWA and Associates, Houston, Texas

JULIAN BRIMELOW

Environment and Climate Change Canada, Edmonton, Alberta, Canada

(Manuscript received 19 July 2019, in final form 22 October 2019)

ABSTRACT

This corrigendum improves upon the size-dependent representation of graupel and hail terminal velocities, kinetic energies, and mass fluxes that were reported in the Heymsfield et al. (2018) study. In particular, representation of these dependencies on diameter over the full range of particle sizes is improved upon by correcting minor errors and by developing representations that cover different size ranges.

1. Introduction

Heymsfield et al. (2018, hereafter H18) developed size-dependent relationships for the terminal velocity (V_t), kinetic energy (KE), and mass flux (MF) of natural and 3D printed graupel and hailstones, drawing on a dataset based on collections of graupel and hail at the ground and measurements of printed replicas in a vertical wind tunnel. Because of a minor computational error, the equations [H18, Eqs. (7) and (8)] that were developed to derive the terminal velocity from the particle diameter (D), and KE [H18, Eq. (10)] and MF [H18, Eq. (13)] from D, as well as the fitting parameters for the power laws for different percentiles given in Table 2 in H18, are in need of a correction. The computational error came about because one of the Interactive Data Language (IDL) structures for graupel particle mass and terminal velocity had omitted one of the data sources for particle mass. This problem, although minor, factored into the calculations for not only graupel but when graupel and hail particles were combined. Accordingly, we have carefully reexamined all aspects of our study and have made slight adjustments to equations where deemed desirable.

Corresponding author: Andrew Heymsfield, heyms1@ucar.edu

DOI: 10.1175/JAS-D-19-0185.1

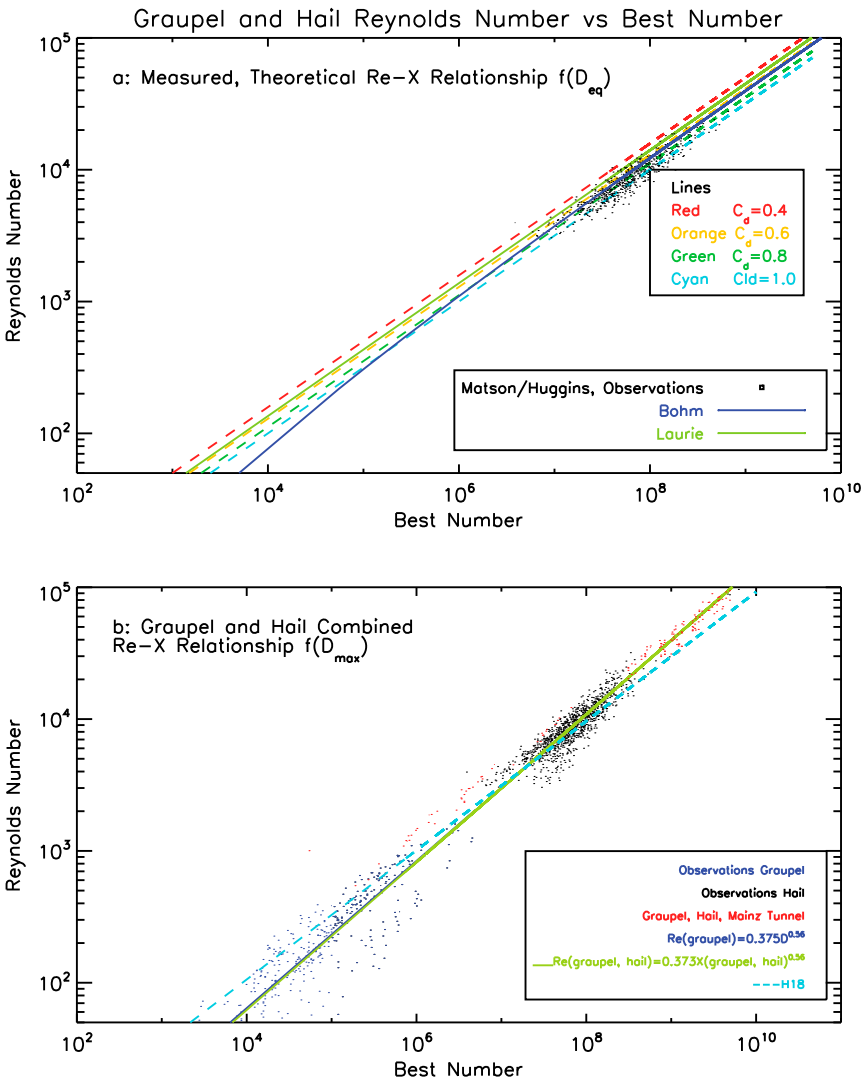

FIG. 1. Reynolds number vs Best number (a) for hail and (b) for the revised dataset, with graupel and hail combined.

2. Results

a. Reynolds number–Best number

Figure 1 shows the revised Reynolds number (Re)–Best number (X) relationship derived from observations and theory. In Fig. 1a, Re–X values that are based on the direct measurements (i.e., observations) of Matson and Huggins (1980), the theoretically based curve of Böhm (1989), and those from the widely used Laurie (1960) study are shown. Figure 1b includes graupel observations from Locatelli and Hobbs (1974), Pflaum (1978), Knight and Heymsfield (1983), and Heymsfield and Kajikawa (1987); observations for hail from Matson and Huggins (1980) and Roos and Carte (1973); and the H18 wind tunnel results, corrected for the identified error previously noted. Table 1 lists the curves for graupel from H18 (row 1), and fitted to the observations for graupel, modified to account for the error in H18 (row 2); the observations for hail (row 3); the hail observations combined with the wind tunnel data (row 4); and the analysis of H18 for graupel combined with hail (row 5). The curves for graupel (387 data points), and graupel and hail combined (1214 points), have almost the same coefficients; because the number of graupel data points weighted the size distribution of the

TABLE 1. Relationships developed between the Reynolds number and Best number, and how well the fitted curves represent the data. The following abbreviations are used: calculated, calc; measured, meas; and observed, obs.

Relationship	Fit	Median ratio Re(calc)/Re(meas)	Mean ratio Re(calc)/Re(meas)	Standard deviation Re(calc)/Re(meas)
Graupel, H18	$\mathrm{Re} = 0.29X^{0.59}$	1.03	1.25	0.76
Graupel, obs only	$\mathrm{Re} = 0.38X^{0.56}$	0.92	1.12	0.68
Hail, obs only	$\mathrm{Re} = 0.41X^{0.56}$	0.98	1.06	0.41
Graupel, hail obs + tunnel	$\mathrm{Re} = 0.37X^{0.56}$	1.13	1.18	0.23
H18 graupel and hail	$\mathrm{Re} = 1.16X^{0.49}$	0.96	1.12	0.61

combined dataset toward the small diameters; this weighting accounted for most of the error.

Metrics for the performance of each curve, given by the ratio of Re as predicted by the fitted curve to Re observed (or observed combined with the wind tunnel–derived values), are shown in Table 1. The combined and H18 relationships both provide good fits to the

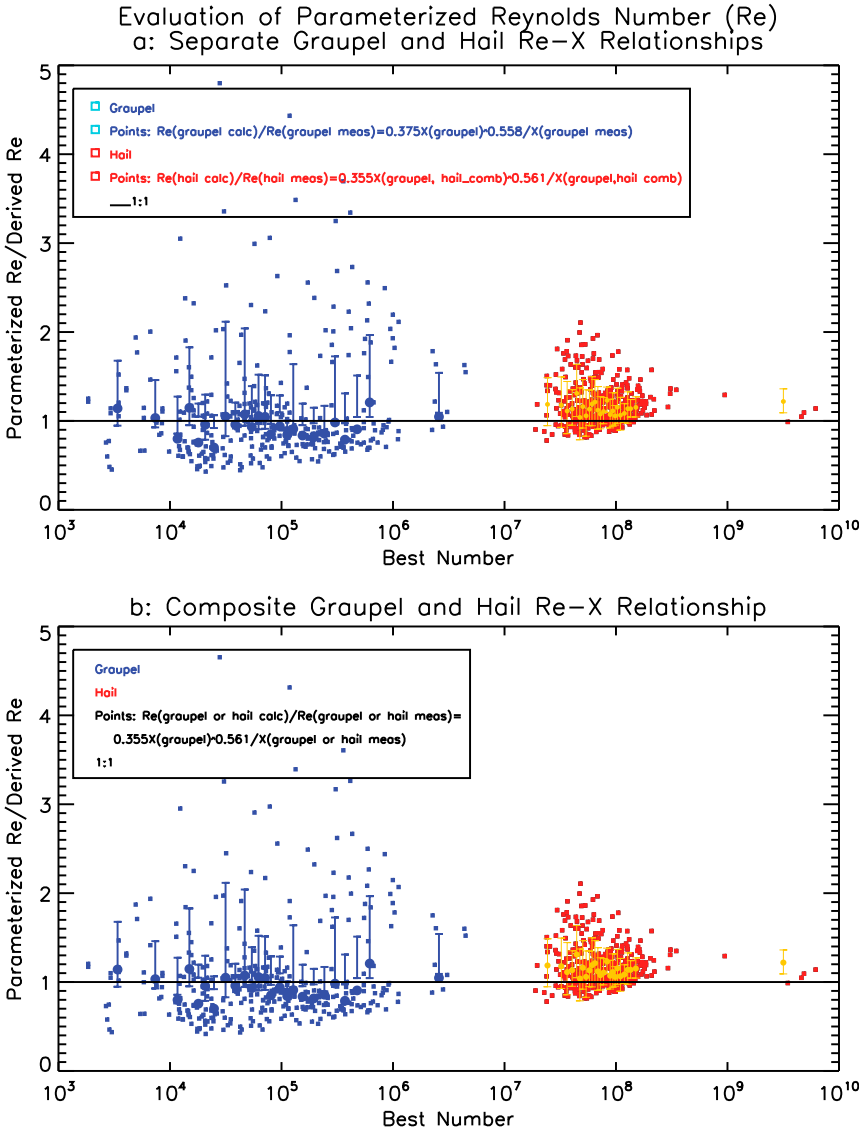

FIG. 2. Evaluation of the quality of the curve fits (a) using the observations for graupel and hail separately and (b) for the combined observations and wind tunnel results.

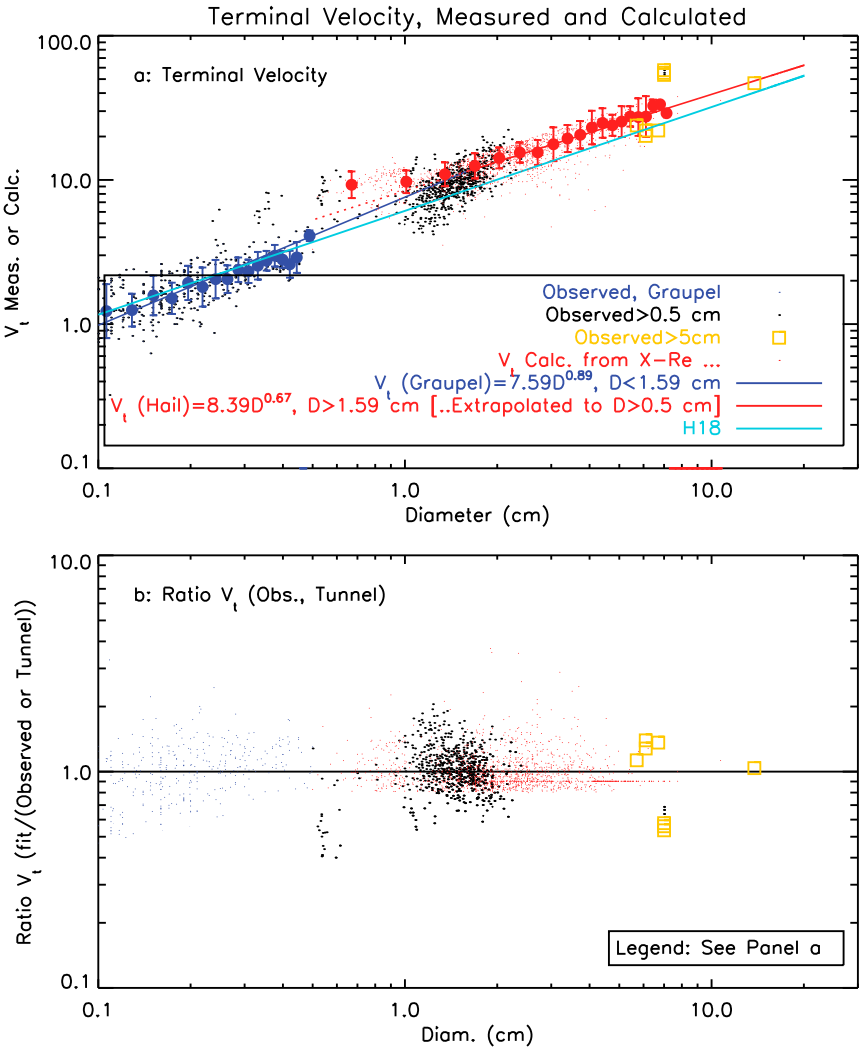

FIG. 3. (a) Observed terminal velocities, or calculated from the wind tunnel measurements using the Re–X relationship [Eq. (1)], as a function of diameter. Different curve fits identified in the text are described and presented in Table 3. (b) Ratio of the terminal velocity calculated from the fit to the observed together with the calculated terminal velocity divided by the observed or calculated terminal velocity, as a function of diameter. Assessment of the quality of each of the fits is summarized in Table 2.

data, but the combined dataset (i.e., observed hail and wind tunnel observations) has a much smaller standard deviation. The graupel and hail relationships for the observed data, shown separately in the table, each provide a good fit.

Figure 2a shows how well the relationships based on the observations for graupel, and the combined observational and wind tunnel data, comply with the data. The results for the combined graupel and hail data differ little from the separate relationships (Fig. 2b). The use of the observations and wind tunnel results combined

$$\mathrm{Re} = 0.38X^{0.56} \tag{1}$$

provides a good fit to the data.

b. *Terminal velocity*

Figure 3a shows the dependence of graupel and hail terminal velocities on their maximum dimension. One set of points is based on the direct physical measurements (observations).

TABLE 2. Relationships developed between the terminal velocity (V_t; m s^{-1}) and diameter (D; cm), and how well the curve fits represent the data.

Relationship	Fit	Median ratio V_t(calc)/V_t(obs)	Mean ratio V_t(calc)/V_t(obs)	Standard deviation V_t(calc)/V_t(obs)
Graupel, H18	$V_t = 6.35D^{0.87}$	0.90	0.91	0.29
Graupel, obs	$V_t = 7.6D^{0.89}$	1.04	1.05	0.33
Graupel, hail, obs	$V_t = 7.2D^{0.84}$	1.02	1.05	0.31
Hail, obs + tunnel (>0.5 cm)	$V_t = 7.6D^{0.89}$ $0.5 < D < 1.59$ cm	1.07	0.93	0.44
	$V_t = 8.4D^{0.67}$ $D > 1.59$ cm	1.04	0.97	0.26
H18 (compared to obs)	$V_t = 6.1D^{0.72}$	0.89	0.95	0.31
H18 (compared to V_t from tunnel)	$V_t = 6.1D^{0.72}$	0.75	0.86	0.32

A second set uses the Re–X relationship [Eq. (1)], with inputs for X (diameter, mass) from the Insurance Institute for Business and Home Safety (IBHS) measurements, to derive V_t. These are

$$V_t = 7.6D^{0.89}, \quad D < 1.5\,\text{cm} \tag{2a}$$

and

$$V_t = 8.4D^{0.67}, \quad D > 1.5\,\text{cm}. \tag{2b}$$

The curve from H18 is plotted for comparison. Note that the new curve for hail conforms better to the larger hailstones than the H18 curve. (See H18 for the data sources for the >5-cm hailstones.) If V_t for graupel only was needed, the single curve extrapolated to $D > 1.5$ cm could readily be used. For both graupel and hail, the two curves, over the respective diameter limits, can be used to estimate V_t.

Table 2 compares fitted curves for graupel and hail for different scenarios, and indicates how well each of the curves fit the respective dataset: the observations for graupel, using the H18 curve (row 1) and the revised curve (row 2); a fit to the observations for graupel and hail combined (row 3); for hail, observed and from the wind tunnel (row 4); and the H18 curve, compared to the observations (row 5) and wind tunnel measurements (row 6). It is noted that the new curve fitted to the observations for graupel more accurately fits the data than the H18 relationship for graupel. A fit to the combined graupel and hail observations match those data extremely well. Our new, two-relationship fit to the observations together with the wind tunnel results also match the data extremely well. They are a significant improvement over the use of the single H18 relationships.

It is important, in our view, for numerical modeling studies to represent the natural variability of the terminal velocities of graupel or hail at any given size. Two particles of the same diameter but different masses or cross-sectional areas are likely to be transported into different regions of an updraft, with consequently different trajectories and growth. For this reason, in Table 3 we provide size-dependent relationships for V_t at percentiles that enclose the population at given sizes (as in H18).

TABLE 3. Power-law fits of terminal velocity (V_t; m s^{-1}) to maximum diameter (D; cm), where $V_t = aD^b$.

Percentile	a coefficient	b coefficient
10th	6.73	0.68
25th	8.33	0.62
50th	9.45	0.62
75th	10.54	0.63
90th	11.58	0.58

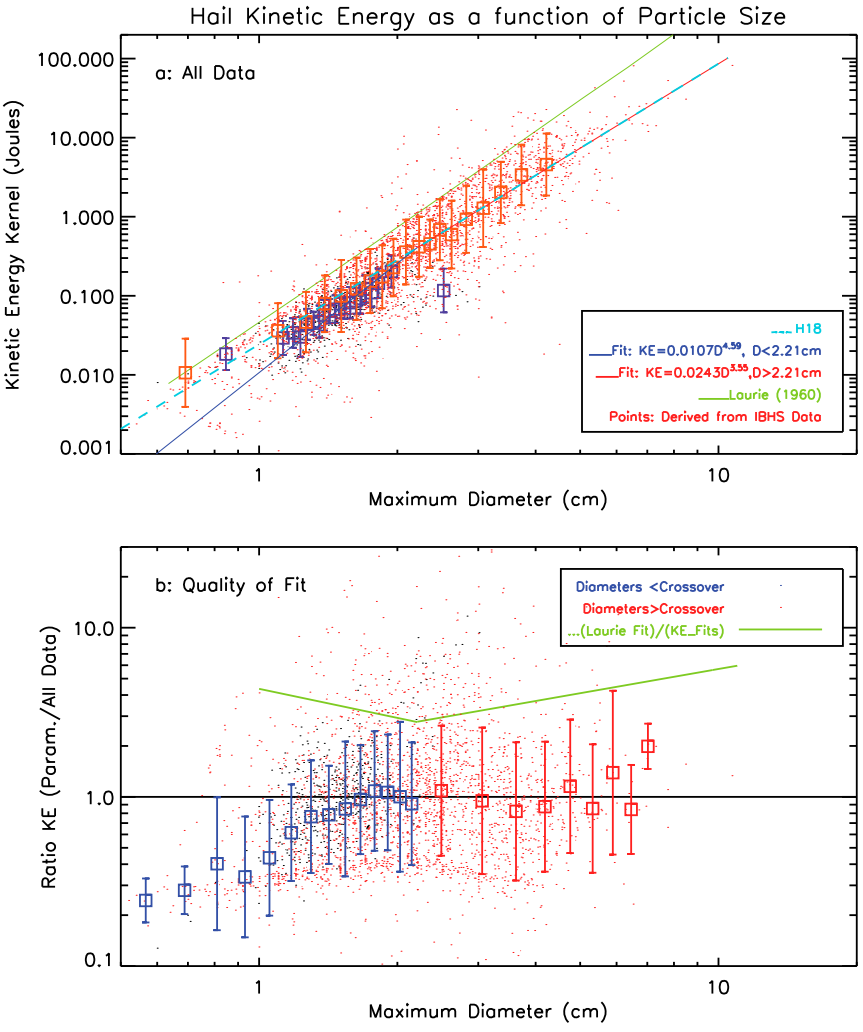

FIG. 4. (a) Kinetic energy for particles of graupel and hail sizes as measured (observed) and also derived from the IBHS mass and cross-sectional area data and the Re–X relationship. Two least squares curves, and the relationships derived, are shown. Also shown is the curve derived from the Laurie (1960) data. (b) Assessment of the quality of each of the fits, with the results summarized in Table 4.

c. *Kinetic energy*

The graupel and hail KE–D relationship of H18 has been reworked to better conform with the revised analysis of the Re–X and V_t–D relationships. Consistent with the latter analysis, two curves were fitted over different size ranges to provide better agreement with both the observations (mainly 1–2 cm) and the wind tunnel results (many with diameters above 2 cm) (Fig. 4a):

$$\mathrm{KE} = 0.0107D^{4.59}, \quad D < 2.21\ \mathrm{cm} \tag{3a}$$

and

$$\mathrm{KE} = 0.0243D^{3.5}, \quad D > 2.21\ \mathrm{cm}. \tag{3b}$$

The H18 relationship is almost identical to the new relationship that was fitted mainly to the wind tunnel measurements for diameters above 2.21 cm, the diameter where the two new relationships cross over. Figure 4b shows how well the new relationships match the

TABLE 4. Relationships developed between graupel and hail kinetic energy (KE; J) and diameter (D; cm), and how well the curve fits represent the measurements (observations), and the measurements + wind tunnel measurements.

Relationship	Fit	Median ratio KE(calc)/KE(obs)	Mean ratio KE(calc)/KE(obs)	Standard deviation KE(calc)/KE(obs)
Measurements: Applied to graupel and hail meas	$KE = 0.0107D^{4.5}$	0.96	1.25	1.31
Measurements: Applied to meas + wind tunnel graupel + hail	$KE = 0.0107D^{4.59}$	1.00	1.50	1.51
Composite relationship [Eqs. (3a) and (3b)]: Applied to meas + wind tunnel graupel + hail	$KE = 0.0107D^{4.59}$ $D < 2.21$ cm $KE = 0.0243D^{3.55}$ $D > 2.21$ cm	1.19	0.96	1.05
Composite relationship [Eqs. (3a) and (3b)]: Applied to meas + wind tunnel	$KE = 0.0107D^{4.59}$ $D < 2.21$ cm $KE = 0.0243D^{3.55}$ $D > 2.21$ cm	1.28	0.84	1.35
H18 Eq. (10) (compared to obs)	$KE = 0.0243D^{3.55}$	1.45	1.74	1.18

TABLE 5. Power-law fits of kinetic energy (KE; J) to maximum diameter (D; cm) in percentiles, where $KE = aD^b$.

Percentile	a coefficient	b coefficient
10th	0.0064	3.75
25th	0.0121	3.73
50th	0.0244	3.55
75th	0.0400	3.63
90th	0.0511	3.80

TABLE 6. Coefficients in mass flux (MF; g cm s^{-1})–diameter (D; cm) power-law relationships, where $MF = aD^b$ at pressure P = 1000 hPa.

Percentile	a coefficient	b coefficient
10th	106.3	3.51
25th	177.2	3.46
50th	275.0	3.41
75th	363.0	3.38
90th	402.6	3.53
Composite	241.0	3.52

observations and wind tunnel results, and Table 4 summarizes the results and compares them with the H18 parameterization. The new curves provide better agreement with the particles at both the smaller and larger diameters. Relative to the new curves, the Laurie relationship produces much larger KE (Fig. 4b).

It is important to represent accurately the KE of hailstones for different diameters when considering the values of KE used in impact testing of materials for hail resistance and for damage modeling. Single power-law fits to the distribution of KE–D for different size percentiles are shown in Table 5. These values are the same as those in H18, except for the 50th percentile.

d. Mass flux

Given the potential importance of the hail precipitation rate, Table 6 shows the fractional distribution of the graupel and hail mass flux as a function of diameter. The results are similar to those in H18.

3. Concluding remarks

This article has developed relationships that relate different properties of graupel and hail to their maximum diameter, drawing on a combination of measurements of natural particles and those printed from 3D scans of natural hailstones. This work corrects a minor problem found in the study by H18, and in so doing improves upon the work reported in that study. Careful attention is given to developing relationships that provide better fits to the data over specific size ranges and to characterizing how well the relationships match the data together with how they improve upon other possible solutions. Further testing is needed in order to more accurately represent the orientation of falling graupel and hail as a factor that alters the terminal velocities of individual hailstones during their fall.

REFERENCES

Böhm, H. P., 1989: A general equation for terminal fall speed of solid hydrometeors. *J. Atmos. Sci.*, **46**, 2419–2427, https://doi.org/10.1175/1520-0469(1989)046<2419:AGEFTT>2.0.CO;2.

Heymsfield, A. J., and M. Kajikawa, 1987: An improved approach to calculating terminal velocities of plate-like crystals and graupel. *J. Atmos. Sci.*, **44**, 1088–1099, https://doi.org/10.1175/1520-0469(1987)044<1088:AIATCT>2.0.CO;2.

——, M. Szakáll, A. Jost, I. Giammanco, and R. Wright, 2018: A comprehensive observational study of graupel and hail terminal velocity, mass flux, and kinetic energy. *J. Atmos. Sci.*, **75**, 3861–3885, https://doi.org/10.1175/JAS-D-18-0035.1.

Knight, N. C., and A. J. Heymsfield, 1983: Measurement and interpretation of hailstone density and terminal velocity. *J. Atmos. Sci.*, **40**, 1510–1516, https://doi.org/10.1175/1520-0469(1983)040<1510:MAIOHD>2.0.CO;2.

Laurie, J. A. P., 1960: Hail and its effects on buildings. Council for Scientific and Industrial Research Rep. 176, 12 pp.

Locatelli, J. D., and P. V. Hobbs, 1974: Fall speeds and masses of solid precipitation particles. *J. Geophys. Res.*, **79**, 2185–2197, https://doi.org/10.1029/JC079i015p02185.

Matson, R. J., and A. W. Huggins, 1980: The direct measurement of the sizes, shapes and kinematics of falling hailstones. *J. Atmos. Sci.*, **37**, 1107–1125, https://doi.org/10.1175/1520-0469(1980)037<1107:TDMOTS>2.0.CO;2.

Pflaum, J. C., 1978: A wind tunnel study on the growth of graupel. Ph.D. dissertation, University of California, Los Angeles, 107 pp.

Roos, D. S., and A. E. Carte, 1973: The falling behavior of oblate and spiky hailstones. *J. Rech. Atmos.*, **7**, 39–52.